

UCLA

UCLA Previously Published Works

Title

In the setting of β -cell stress, the pancreatic duct gland transcriptome shows characteristics of an activated regenerative response

Permalink

<https://escholarship.org/uc/item/87z0m3pr>

Journal

AJP Gastrointestinal and Liver Physiology, 315(5)

ISSN

0193-1857

Authors

Butler, Alexandra E
Kirakossian, David
Gurlo, Tatyana
[et al.](#)

Publication Date

2018-11-01

DOI

10.1152/ajpgi.00177.2018

Peer reviewed

1 **In the Setting of Beta Cell Stress, the Pancreatic Duct Gland Transcriptome**
2 **Shows Characteristics of an Activated Regenerative Response**

3 Running Title: Pancreatic duct glands

4

5 **Alexandra E. Butler¹, David Kirakossian¹, Tatyana Gurlo¹, Fuying Gao², Giovanni**
6 **Coppola², Peter C. Butler¹**

7 ¹Larry L. Hillblom Islet Research Center, David Geffen School of Medicine, University of
8 California Los Angeles, Los Angeles, California ²Department of Psychiatry, Semel
9 Institute for Neuroscience and Human Behavior, David Geffen School of Medicine,
10 University of California Los Angeles, Los Angeles, California

11

12 **CORRESPONDENCE** and reprint requests to:

13 Peter C. Butler, MD

14 Larry L. Hillblom Islet Research Center

15 UCLA David Geffen School of Medicine

16 900 Veteran Ave, 24-130 Warren Hall

17 Los Angeles CA 90095-7073, USA

18 Tel +1 310 794 7645

19 Fax +1 310 206 5368

20 Email: pbutler@mednet.ucla.edu

21

22 **ABSTRACT**

23 The pancreatic duct gland (PDG) compartment has been proposed as a potential stem
24 cell niche based on its coiled tubular structure embedded in mesenchyme, its
25 proliferation and expansion in response to pancreatic injury, and the fact that it contains
26 endocrine and exocrine epithelial cells. Little is known of the molecular signature of the
27 PDG compartment in either a quiescent state or the potentially activated state during
28 beta cell stress characteristic of diabetes. To address this, we performed RNA
29 sequencing on RNA obtained from PDGs of wild type versus pre-diabetic HIP rats, a
30 model of type 2 diabetes. The transcriptome of the PDG compartment, compared to a
31 library of 84 tissue types, placed PDGs midpoint between the exocrine and endocrine
32 pancreas and closely related to seminiferous tubules, consistent with a role as a stem
33 cell niche for the exocrine and endocrine pancreas. Standard differential expression
34 analysis (permissive threshold $p < 0.005$) identified 245 genes differentially expressed in
35 PDGs from HIP rats versus WT rats, with overrepresentation of transcripts involved in
36 acute inflammatory responses, regulation of cell proliferation, and tissue development,
37 while pathway analysis pointed to enrichment of cell movement-related pathways. In
38 conclusion the transcriptome of the PDG compartment is consistent with a pancreatic
39 stem cell niche that is activated by ongoing beta cell stress signals. The documented
40 PDG transcriptome provides potential candidates to be exploited for lineage tracing
41 studies of this as yet little investigated compartment.

42

43 **NEW & NOTEWORTHY**

44 The pancreatic duct gland (PDG) compartment has been proposed as potential stem
45 cell niche. Transcriptome analysis of the PDG gland placed it midpoint between
46 exocrine and endocrine tissues with adaptation towards response to inflammation and
47 increased cell movement in a model of type 2 diabetes with ongoing beta cell apoptosis.
48 These findings support the proposal that PDGs may act as a pancreatic stem cell niche.

49

50 **KEYWORDS**

51 Pancreatic duct glands, regeneration, pancreas, endocrine, diabetes

52

53 **GLOSSARY**

54 LCM, laser capture microdissection; OCT, optimum cutting temperature; PDGs,
55 pancreatic duct glands; PEN, polyethylene naphthalate; RNase, ribonuclease; RNA
56 Seq, RNA Sequencing

57

58 INTRODUCTION

59 It has been known for many years that there are glandular-like structures arising from
60 larger pancreatic ducts that undergo proliferation following pancreatic injury with an
61 increase in cells expressing the transcription factor Pdx-1, and containing occasional
62 endocrine cells (22, 23). More recently, these glandular structures were proposed as
63 being a distinct anatomic compartment with molecular features consistent with a stem
64 cell niche, and named pancreatic duct glands (PDGs) (20). PDGs are crypt-like
65 invaginations off the pancreatic ductal tree, embedded in mesenchyme and as such are
66 anatomically reminiscent of the gastric, ileal and colonic crypt stem cell niches (Figure
67 1) (3). Similar glandular structures (peribiliary glands) are present as crypt-like
68 outpouches off the biliary tree and have been reported to bear multiprogenitor cells with
69 a potential ductal epithelium or endocrine fate (8). PDGs, like ileal crypts, have zones of
70 increased replication, consistent with a transit amplifying zone, and a predominance of
71 exocrine epithelial cells with a minority of endocrine cells. The PDG compartment is
72 expanded with increased proliferation in humans with both type 1 diabetes (17) and type
73 2 diabetes (19).

74

75 Relatively little is known about the molecular signature of PDGs. Thus far, molecular
76 characterization of PDGs has relied on candidate immunohistochemistry or RT-PCR in
77 rats or mice (20, 22, 23) and immunohistochemistry in humans (17). To date this
78 approach has revealed Pdx-1, nestin, mucin-6, Hes1 and Ngn3 expression in rodent
79 PDGs and Sox9, GATA4, NKx6.1, NKx2.2 and chromogranin A in humans PDGs.

80

81 Powerful new tools are available to characterize the molecular signatures of tissues of
82 interest based on RNA and/or protein profiling. Laser capture microdissection (LCM) is
83 a technique that enables isolation of RNA and/or protein from a compartment of interest
84 within an organ. After identification of the compartment by microscopy, laser dissection
85 is used to procure a sample of the cells of interest to permit subsequent gene
86 expression and/or proteome profiling (11, 21). In the present study we employed that
87 approach to procure high quality RNA by a protocol validated for PDGs (7). We then
88 characterized the transcriptional profile of these samples using RNA sequencing (RNA-
89 seq) to establish the molecular identity of the PDG compartment in an unbiased
90 manner. We used these data 1) to compare the molecular signature of PDGs to that of
91 multiple tissues; 2) to identify possible markers overrepresented in the PDG
92 compartment; and 3) to compare PDG samples from a rat model of type 2 diabetes (HIP
93 rat) compared to wild type controls, with the goal of identifying the signaling networks
94 and pathways altered in PDGs in the context of diabetes.

95

96 **MATERIALS AND METHODS**

97 **Rats.** The generation of the human IAPP transgenic rats (HIP) has been described in
98 detail previously (5). Wild type rats were littermates of HIP rats. Rats were bred at the
99 University of California, Los Angeles (UCLA) animal housing facility and subjected to a
100 standard 12-h light-dark cycle and were fed Rodent Diet 8604 (Harlan Teklad, Madison,
101 WI) ad libitum. All experimental procedures were approved by the UCLA Institutional
102 Animal Care and Use Committee. HIP rats develop overt diabetes between 9 and 12
103 months of age with islet pathology similar to humans with type 2 diabetes, specifically

104 ongoing beta cell apoptosis with a progressive defect in beta cell mass (5). HIP rats
105 used for this study were ~6 months of age, and so prediabetic with ongoing beta cell
106 apoptosis but without the confounding secondary actions of hyperglycemia on gene
107 expression (15). WT rats were age-matched.

108

109 ***Tissue procurement and LCM.*** On the day of study, animals were anesthetized by
110 inhalation of isoflurane (Abbott Laboratories, Chicago, IL). Rat pancreas was rapidly
111 dissected, divided into two portions (head and body of pancreas, and tail of pancreas),
112 and cryopreserved in Optimal Cutting Temperature (OCT) compound (7). 10-15
113 Sections were cut from the head of the pancreas for each LCM experiment. In brief,
114 eight micrometer sections were mounted on UV irradiated polyethylene naphthalate
115 (PEN) membrane slides and stored at -80°C. Right before use, slides were fixed in
116 alcohol and stained with hematoxylin (solutions contained RNA inhibitors).

117

118 The PDG compartment was identified morphologically. As described in (20, 24), the
119 PDG compartment is readily identifiable in mouse and human pancreas due to its
120 unique architecture distinct from the ductal epithelium. We confirmed previously that
121 similar to humans and mice, PDGs in rat pancreatic tissue sections appear as coiled
122 structures embedded in the mesenchyme surrounding the main duct, and are readily
123 stained with Alcian blue and p-aminosalicylic acid, and also characterized by the
124 increased proliferation rate relative to normal ductal cells (12). For current study we set
125 out to collect only PDGs in the substantial layer of mesenchyme where, based on

126 extensive experience (6, 12, 17, 19), they are readily and rapidly identified, ensuring
127 specificity and quality of collected RNA.

128

129 The PDG compartment was cut into 0.5 ml tube cap (Axygen Scientific Inc, Union City,
130 CA) filled with 10 μ l of extraction buffer (PicoPure[®] RNA Isolation Kit, KIT0204) and 0.5
131 μ l RNase inhibitor (1 U/ μ l) (SUPERase•IN™, AM2694; Ambion[®] Carlsbad, CA). To
132 avoid RNA degradation, slides were processed one at a time, and staining and
133 dissection from each slide was finished within 20 min. The LCM procedure was
134 performed using a LMD7000 Laser Microdissection system (Leica; Wetzlar, Germany)
135 at the California Nano Systems Institute Advanced Light Microscopy/Spectroscopy
136 Shared Resource Facility at UCLA.

137

138 **Quality control and LCM selectivity.** RNA quality was tested with a 2100 Bioanalyzer
139 using a RNA 6000 Pico LabChip Kit (Agilent Technologies, Santa Clara, CA). To
140 validate the LCM selectivity, RNA was isolated from LCM-derived samples from PDGs
141 and islets and tested by RT-PCR for the abundance of transcripts known to be
142 expressed in PDGs or islets. mRNA expression of PDG/ductal cell protein Cytokeratin-
143 19 (CK-19) and islet hormones insulin and glucagon were analyzed (7). By this
144 approach, CK-19 was highly expressed in PDGs but not islets. Insulin and glucagon
145 transcripts were abundantly expressed in islets and at low levels (~1,000 fold lower than
146 islets) in PDGs, consistent with occasional endocrine cells in this compartment. In this
147 study, we ranked expression levels of all 15,679 rat probes included in the RNA-seq
148 annotation and calculated the corresponding expression percentile. Cytokeratin 19

149 (*Krt19*) ranked 6/15,679 (<0.1th percentile), insulin (*Ins1*), ranked 19, 0.1%
150 percentile), *Ins2* ranked #126, 0.7th percentile, and glucagon ranked 13,682 (87th
151 percentile). While Cytokeratin 19 and Glucagon levels were consistently at the top and
152 bottom of the list, respectively, insulin values were more variable across replicates,
153 suggesting variability across our samples. Since we did not run RNAseq on islet tissue
154 for this experiment we cannot assess expression relative to islet tissue.

155

156 **RNA Seq.** RNA-seq was performed in the UCLA Neuroscience Genomics Core (UNGC,
157 <http://www.semel.ucla.edu/ungc>). Between 5-20 ng of total RNA were extracted per
158 tissue. After quantification and quality check, 5 ng of total RNA were amplified at UNGC
159 using the NuGEN Ultralow Library System kit (NuGEN), which is optimized for
160 downstream Illumina library preparation. We extracted RNA from 6 samples: 3 from HIP
161 and 3 from WT animals. Illumina RNA-seq libraries were then prepared according to
162 manufacturer's instructions. Sequencing was performed using the Illumina HiSeq 2500
163 sequencer and the v3 Illumina chemistry. We barcoded multiple samples and ran them
164 over multiple lanes, in order to minimize batch effects (2). We ran the equivalent of 3
165 samples per lane, with paired-end 100bp read length, corresponding to 2 HiSeq 2500
166 lanes.

167

168 Between 83 and 187 million, 100 basepair long, paired-end reads were obtained and
169 aligned to the rat genome (rn5) using the STAR spliced read aligner (10). 65-72% reads
170 mapped uniquely to the rat genome, and ~50% of the genes in the rat genome were
171 detected as present by at least 100 mapping reads. Samples were clustered using

172 hierarchical clustering and multidimensional scaling (MDS), and no outliers were
173 detected.

174

175 **Data Analysis.** An RNA-Seq pipeline is established in the UCLA Informatics Center for
176 Neurogenetics and Neurogenomics (<https://github.com/icnn/RNAseq-PIPELINE.git>).
177 Initial analysis steps included: 1) Quality analysis, alignment to reference genome using
178 STAR (10), and filtering of reads not uniquely mapping or mapping to repetitive regions;
179 2) Mapping of reads to exons, untranslated regions (UTRs) and intron-exon junctions
180 using STAR, and generation of RefSeq isoform counts; 3) Normalization and differential
181 expression analysis by tissue and condition using the software DEseq (1) and edgeR
182 (18); 4) Data upload onto our web-based gene expression database.

183

184 Multidimensional scaling (MDS) was used to cluster PDG samples with samples
185 obtained from an atlas of gene expression in human tissues. Briefly, the human GNF
186 database was downloaded from the bioGPS website (<http://biogps.org>), probes
187 targeting transcripts shared across the two platforms (Affymetrix, used in the GNF
188 database and RNA-seq, used in this study) were normalized jointly using quantile
189 normalization and MDS plots were generated to organize samples in a 2-dimensional
190 space, based on the expression of the top 1000 most variable genes. Differential
191 expression analysis was performed to compare HIP and WT samples, using the edgeR
192 package and setting p-value threshold of 0.005. Gene ontology and pathway analysis
193 were performed using DAVID (<http://david.abcc.ncifcrf.gov/>) and Ingenuity Pathway
194 Analysis (ingenuity.org).

195

196 **RESULTS**

197 ***Identification of the PDG compartment.*** PDGs share many properties with human
198 ileal crypts (Figure 1). Both are crypt like structures embedded in mesenchyme. Ileal
199 crypts and PDGs are composed primarily of gut or pancreas epithelium respectively but
200 with occasional endocrine cells (Figure 1A, 1B). Both ileal crypts and PDGs have zones
201 of increased replication (Figure 1C, 1D). In human and rat pancreas PDGs were readily
202 identified in hematoxylin-stained tissue sections based on their unique anatomic
203 location as invaginations off main pancreatic ducts embedded as coiled structures
204 within the mesenchyme surrounding main pancreatic ducts (Figure 1, 2). In keeping with
205 prior descriptions (12, 19, 20, 24), PDGs were notable for abundant mucins as detected
206 by Alcian Blue, increased frequency of proliferating cells (Figure 1A, 1B) and the
207 presence of occasional insulin positive cells (Figure 1B, 2B).

208

209 ***RNA sequencing-based gene expression analyses in dissected PDG samples.***

210 Having previously established a method to obtain RNA by LCM from PDGs of a suitable
211 quality and confirmed to reflect the PDG compartment based on RT-PCR of sentinel
212 genes (7), we applied this approach here to obtain RNA from PDGs to perform RNA-
213 seq so as to obtain an unbiased genetic expression profile of the PDG compartment.
214 With these data, we then compared the PDG transcriptome to an atlas of transcriptional
215 data including 84 tissues. MDS analysis (see Methods, Figure 3 legend) clustered
216 related tissues (e.g. brain regions, or blood cell types) together due to similarity of their
217 transcriptome. Our PDG samples were placed in a region including other pancreatic

218 samples (both exocrine and endocrine), further supporting their source tissue of origin,
219 but also testis (including seminiferous tubules, which host actively replicating cells with
220 pluripotent potential), and pituitary gland (Figure 3).

221
222 We then proceeded to identify the markers most specific to the PDG compartment.
223 Briefly, after normalization we compared the all six PDG samples to the average of all
224 other tissues in the GNF database. This analysis identified 22 transcripts as putatively
225 overexpressed in PDG cells relative to the average expression levels of 84 tissues
226 ($p < 0.005$, Table 1). Finally, we compared PDG expression profiles between HIP and
227 WT rats (Table 2). Standard differential expression analysis at a permissive threshold
228 ($p < 0.005$) identified 245 genes (Figure 4A, 4B), which were differentially expressed
229 across the three replicates. Gene Ontology analysis (Figure 4C) highlighted an
230 overrepresentation of transcripts involved in acute inflammatory response, regulation of
231 cell proliferation, and tissue development. Pathway analysis pointed to enrichment of
232 cell movement-related pathways, and the top 2 networks (Figure 5A, 5B) included
233 *ADIPOQ*, playing an important role in type 2 diabetes, and the known therapeutic target
234 *PPARG*.

235
236 In conclusion, unbiased transcriptional analyses support the notion that the PDG
237 compartment includes a unique transcriptional niche, similar to both the tissue of origin
238 (pancreas) and to replicating cells, and that a signal related to diabetes is detectable in
239 a rat model of type 2 diabetes.

240

241 **DISCUSSION**

242 While the existence of blind pouches from main pancreatic ducts bearing stem cell
243 markers has been appreciated for many years, only recently has this anatomical
244 compartment been named the pancreatic duct gland (PDG) compartment and been
245 proposed as a stem cell niche responsible for repair of pancreas following acute injury
246 (20).

247

248 Features of the PDG compartment that are consistent with a stem cell niche include a
249 tubular crypt like structure embedded in mesenchyme, expression of stem cell markers
250 such as Hes-1 and proliferation with expansion in response to inflammation and/or
251 injury (20). Other foregut derived tissues such as the duodenum and proximal ileum
252 have well-characterized stem cell niches that are also crypt-like, located at the base of
253 the intestinal villi embedded in mesenchyme. These well-defined stem cell niches
254 generate cells that transition through proliferative transit amplifying zones to generate
255 sufficient cells to replace the short-lived epithelial cells that migrate up the villi and are
256 discarded after several days. A small subset of cells (~1%) derived from the intestinal
257 crypt are transdifferentiated into endocrine cells under the induction of Ngn-3 signaling
258 (9). This raises the possibility that the PDG compartment might not only serve to repair
259 exocrine ductal tissue as already reported, but also be a potential source of pancreatic
260 endocrine cells, although no effective beta cell formation from the PDG compartment
261 was identified in humans with type 1 or 2 diabetes (17, 19).

262

263 The turnover of pancreatic duct epithelial cells is much less frequent than that of the
264 cells that form intestinal villi. However, in common with intestinal crypts, PDGs have a
265 zone of increased replication compared to that of the duct epithelia, and this is
266 enhanced in response to injury or the known growth factor GLP-1 (12) (19). The
267 unbiased gene expression studies by RNA-seq of PDGs presented in this manuscript
268 reveal a molecular signature intermediate between the exocrine and endocrine
269 pancreas as well as the well-defined stem cell niche in the testis, consistent with a
270 pancreatic stem cell niche that may serve both the exocrine and endocrine pancreas.

271

272 There has been controversy as to whether endocrine cells arise from pancreatic duct
273 epithelium in postnatal life (so called ductal neogenesis) (13). The postulate that they do
274 was initially rendered based on the adjacency of islets and pancreatic duct epithelium
275 commonly found in pancreas (4). However, most lineage studies have failed to
276 demonstrate endocrine cells arising from pancreatic ductal or acinar cells. One possible
277 explanation for this is that the lineage markers employed represent those of definitive
278 ductal epithelium rather than that of the putative pancreatic stem cell niche. One of the
279 purposes of the present study was to further characterize the molecular identity of the
280 PDG compartment to offer investigators potential candidates to lineage trace the
281 derivatives of the compartment. Several lines of investigation suggest that there is
282 ongoing beta cell formation in the adult pancreas that cannot be attributed only to
283 replication of existing beta cells (16).

284

285 Modeling studies applied to the HIP rat model of type 2 diabetes revealed an adaptive
286 increase in beta cell formation not attributable to beta cell replication (14). Therefore, we
287 selected this model of type 2 diabetes to investigate the PDG transcriptome for
288 evidence of adaptive changes that might be expected in a relevant stem cell niche.
289 Differential gene expression analysis between PDGs from HIP and WT rats were
290 consistent with tissue stem cell response to injury in a relevant compartment. For
291 example the most significant alteration was in genes engaged in inflammatory
292 responses. This implies communication between injured pancreatic islets and PDGs,
293 presumably either through the known intrapancreatic portal venous system or through
294 the rich intrapancreatic neural network. Also, given the well-recognized role that
295 inflammatory pathways play in the induction of tissue repair, it is of interest that PDGs in
296 HIP rats not only apparently sense and respond to pancreatic islet inflammation, but
297 also that regulation of cell proliferation and tissue development genes are also highly
298 represented in the PDG transcriptome of HIP rats compared to non-diabetic WT rats.
299 Pathway analysis also pointed to enrichment of cell movement-related pathways, and
300 the top 2 networks (Figure 5A, 5B) included *ADIPOQ*, a gene with known linkage to
301 obesity and type 2 diabetes, and the therapeutic target in type 2 diabetes, *PPARG*. The
302 PDG compartment has been reported to be expanded with increased proliferation in
303 humans with both type 1 and 2 diabetes, and this is reproduced in the HIP rat model
304 (17, 19). Here we now report the transcriptome of the PDG is consistent with a tissue
305 stem cell niche serving both the exocrine and endocrine pancreas, and undergoing
306 anticipated adaptive changes in response to inflammatory signals arising from stressed
307 beta cells.

308

309 If the PDG compartment is a potential source of new beta cells, the question arises, why
310 are beta cells not restored in type 1 and 2 diabetes? Tissue stem cell niches
311 recapitulate the development of the host tissue, and so endocrine cells would be
312 expected to be a minority of new cells formed by a pancreatic stem cell niche.
313 Moreover, in the face of ongoing beta cell autoimmunity in type 1 diabetes, and
314 misfolded protein stress in type 2 diabetes, presumably beta cell loss would likely match
315 any beta cell formation. On the other hand if the PDG compartment can serve as a
316 source of new beta cells, it is plausible that the relative fate of newly forming cells might
317 be therapeutically manipulated towards an endocrine rather than exocrine fate to
318 enhance new cell formation.

319

320 As with all studies, the present studies have limitations. The samples sizes are relatively
321 small, constrained by the costs of the dissection protocol and RNA seq. The studies are
322 limited to rodent pancreas, as efforts to procure consistently high quality RNA from
323 human pancreas samples unfortunately were unsuccessful. Nonetheless the data that
324 has been established implies that the PDG compartment may indeed serve as a
325 pancreatic stem cell niche, and provides some insights that might be exploited to
326 establish lineage dynamics in genetic models.

327

328 **ACKNOWLEDGMENTS**

329 We appreciate the editorial assistance of Bonnie Lui, from the Hillblom Islet Research
330 Center at UCLA. This research was performed with the support of the Network for
331 Pancreatic Organ Donors with Diabetes (nPOD), a collaborative type 1 diabetes
332 research project sponsored by the Juvenile Diabetes Research Foundation International
333 (JDRF). Organ Procurement Organizations (OPO) partnering with nPOD to provide
334 research resources are listed at www.jdrfnpod.org/our-partners.php. We acknowledge
335 the support of the NINDS Informatics Center for Neurogenetics and Neurogenomics
336 (P30 NS062691) and Charles Blum for technical assistance. We acknowledge the CNSI
337 Advanced Light Microscopy/Spectroscopy Facility at California Nanosystems Institute,
338 UCLA for help with the LCM experiments.

339

340 **GRANTS**

341 The work was supported by NIH/NIDDK DK077967, Larry L. Hillblom Foundation (2014-
342 D-001-NET).

343

344 **DISCLOSURES**

345 The authors have no conflicts of interest.

346

347 **AUTHOR CONTRIBUTIONS**

348 AEB and DK performed the experiments, AEB, TG, GC and PCB designed the studies
349 and helped write the manuscript, FG and GC performed the analysis of the RNA-seq
350 pathways and networks.

351 **FIGURE LEGENDS**

352 **Figure 1. Comparison of pancreatic duct gland and ileal crypt.**

353 Human ileal crypts and PDGs share many properties. Both are crypt like structures
354 embedded in mesenchyme (A, B). Ileal crypts and PDGs are composed primarily of gut
355 or pancreas epithelium respectively but with occasional endocrine cells (A, inset stained
356 brown, chromogranin) and (B, stained pink, insulin). Both ileal crypts and PDGs have
357 zones of increased replication (Ki67 C, D) compared to surrounding structures,
358 consistent with a role as a transit amplifying zone. The variability in frequency of
359 proliferating cells in PDG compartments was detected.

360

361 **Figure 2. Pancreatic duct gland histology.**

362 A. Section through a large duct in pancreas from a wild type [WT] rat demonstrating the
363 pancreatic duct gland [PDG] compartment present in the mesenchyme surrounding the
364 large duct, with PDGs connecting directly with the large duct lumen (arrows). B. Section
365 through a large duct in pancreas from a human IAPP transgenic [HIP] rat demonstrating
366 the extensive pancreatic duct gland [PDG] compartment relative to WT rats. Sections
367 are stained for insulin [DAB] with hematoxylin counterstain. Images were taken at 10x
368 (100x magnification). ★ indicates large duct lumen. The inset (B) shows a PDG epithelial
369 cell staining for insulin. Scale bar= 200µm.

370

371 **Figure 3. Multidimensional scaling plot of tissue samples human expression atlas**

372 (<http://biogps.org/>). Each dot represents the relative location of gene profile from one
373 of the 176 samples from 84 surveyed tissues. Dots are color-coded by tissue group or

374 system. Samples cluster based on similarity. Validity of the analytical approach is
375 illustrated by the clustering of expression profiles obtained for brain or blood (shades
376 areas). In red, RNA-seq-derived genetic profiles obtained from PDGs are reassuringly
377 close to each other. Also, PDG gene expression profiles are placed between a classical
378 stem cell profile (germ cells) and stem cell niche profile (Leydig cells) in one dimension
379 and then close to the two pancreas compartments (islet and exocrine pancreas).

380

381 **Figure 4. Differential expression analysis comparing PDG samples from HIP and**
382 **WT rats.** (A) Number of up- (red bar) and down-regulated (green) transcripts when
383 comparing HIP vs. WT; (B) heatmap representing ratios of the 245 dysregulated
384 transcripts. Individual genes are in rows, samples are in columns. Each cell represents
385 a ratio (each HIP sample vs. the average of WT). Shades of red: upregulation, shades
386 of green: downregulation; (C) overrepresentation of gene ontology categories within the
387 differentially expressed gene set. Within each category, green represents the proportion
388 of downregulated and red the portion of upregulated transcripts when comparing HIP
389 vs. WT samples.

390

391 **Figure 5.** Top two networks identified by Ingenuity Pathway Analysis as
392 overrepresented within the list of 245 genes ($p < 0.005$) dysregulated in HIP vs. WT.
393 Symbols in shades of green or red denote up- and down-regulated transcripts,
394 respectively. Symbols in gray are not significantly differentially expressed in this
395 dataset, but known to be part of the pathway or network. Solid lines denote direct

396 interaction, dotted lines indirect interaction, such as an alteration in expression levels, or
397 post-translational modification.

398 REFERENCES

- 399 1. **Anders S, and Huber W.** Differential expression analysis for sequence count
400 data. *Genome Biol* 11: R106, 2010.
- 401 2. **Auer PL, and Doerge RW.** Statistical design and analysis of RNA sequencing
402 data. *Genetics* 185: 405-416, 2010.
- 403 3. **Barker N, Bartfeld S, and Clevers H.** Tissue-resident adult stem cell
404 populations of rapidly self-renewing organs. *Cell Stem Cell* 7: 656-670, 2010.
- 405 4. **Bonner-Weir S, Toschi E, Inada A, Reitz P, Fonseca SY, Aye T, and Sharma
406 A.** The pancreatic ductal epithelium serves as a potential pool of progenitor cells.
407 *Pediatr Diabetes* 5 Suppl 2: 16-22, 2004.
- 408 5. **Butler AE, Jang J, Gurlo T, Carty MD, Soeller WC, and Butler PC.** Diabetes
409 due to a progressive defect in beta-cell mass in rats transgenic for human islet
410 amyloid polypeptide (HIP Rat): a new model for type 2 diabetes. *Diabetes* 53:
411 1509-1516, 2004.
- 412 6. **Butler AE, Matveyenko AV, Kirakossian D, Park J, Gurlo T, and Butler PC.**
413 Recovery of high-quality RNA from laser capture microdissected human and
414 rodent pancreas. *J Histotechnol* 39: 59-65, 2016.
- 415 7. **Butler AE, Matveyenko AV, Kirakossian D, Park J, Gurlo T, and Butler PC.**
416 Recovery of high quality RNA from laser capture microdissected human and
417 rodent pancreas. *Journal of Histotechnology* In Press, 2015.
- 418 8. **Carpino G, Cardinale V, Onori P, Franchitto A, Berloco PB, Rossi M, Wang
419 Y, Semeraro R, Anceschi M, Brunelli R, Alvaro D, Reid LM, and Gaudio E.**
420 Biliary tree stem/progenitor cells in glands of extrahepatic and intraheptic bile
421 ducts: an anatomical in situ study yielding evidence of maturational lineages.
422 *Journal of anatomy* 220: 186-199, 2012.
- 423 9. **Cortina G, Smart CN, Farmer DG, Bhuta S, Treem WR, Hill ID, and Martin
424 MG.** Enteroendocrine cell dysgenesis and malabsorption, a histopathologic and
425 immunohistochemical characterization. *Hum Pathol* 38: 570-580, 2007.
- 426 10. **Dobin A, Davis CA, Schlesinger F, Drenkow J, Zaleski C, Jha S, Batut P,
427 Chaisson M, and Gingeras TR.** STAR: ultrafast universal RNA-seq aligner.
428 *Bioinformatics* 29: 15-21, 2013.
- 429 11. **Emmert-Buck MR, Bonner RF, Smith PD, Chuaqui RF, Zhuang Z, Goldstein
430 SR, Weiss RA, and Liotta LA.** Laser capture microdissection. *Science* 274: 998-
431 1001, 1996.
- 432 12. **Gier B, Matveyenko AV, Kirakossian D, Dawson D, Dry SM, and Butler PC.**
433 Chronic GLP-1 receptor activation by exendin-4 induces expansion of pancreatic
434 duct glands in rats and accelerates formation of dysplastic lesions and chronic
435 pancreatitis in the Kras(G12D) mouse model. *Diabetes* 61: 1250-1262, 2012.
- 436 13. **Kushner JA, Weir GC, and Bonner-Weir S.** Ductal origin hypothesis of
437 pancreatic regeneration under attack. *Cell Metab* 11: 2-3, 2010.

- 438 14. **Manesso E, Toffolo GM, Saisho Y, Butler AE, Matveyenko AV, Cobelli C,**
439 **and Butler PC.** Dynamics of beta-cell turnover: evidence for beta-cell turnover
440 and regeneration from sources of beta-cells other than beta-cell replication in the
441 HIP rat. *Am J Physiol Endocrinol Metab* 297: E323-330, 2009.
- 442 15. **Matveyenko AV, and Butler PC.** Beta-cell deficit due to increased apoptosis in
443 the human islet amyloid polypeptide transgenic (HIP) rat recapitulates the
444 metabolic defects present in type 2 diabetes. *Diabetes* 55: 2106-2114, 2006.
- 445 16. **Meier JJ, Bhushan A, Butler AE, Rizza RA, and Butler PC.** Sustained beta cell
446 apoptosis in patients with long-standing type 1 diabetes: indirect evidence for
447 islet regeneration? *Diabetologia* 48: 2221-2228, 2005.
- 448 17. **Moin AS, Butler PC, and Butler AE.** Increased Proliferation of the Pancreatic
449 Duct Gland Compartment in Type 1 Diabetes. *J Clin Endocrinol Metab* 102: 200-
450 209, 2017.
- 451 18. **Robinson MD, McCarthy DJ, and Smyth GK.** edgeR: a Bioconductor package
452 for differential expression analysis of digital gene expression data. *Bioinformatics*
453 26: 139-140, 2010.
- 454 19. **Schludi B, Moin ASM, Montemurro C, Gurlo T, Matveyenko AV, Kirakossian**
455 **D, Dawson DW, Dry SM, Butler PC, and Butler AE.** Islet inflammation and
456 ductal proliferation may be linked to increased pancreatitis risk in type 2 diabetes.
457 *JCI insight* 2: 2017.
- 458 20. **Strobel O, Rosow DE, Rakhlin EY, Lauwers GY, Trainor AG, Alsina J,**
459 **Fernandez-Del Castillo C, Warshaw AL, and Thayer SP.** Pancreatic duct
460 glands are distinct ductal compartments that react to chronic injury and mediate
461 Shh-induced metaplasia. *Gastroenterology* 138: 1166-1177, 2010.
- 462 21. **Suarez-Quian CA, Goldstein SR, Pohida T, Smith PD, Peterson JI, Wellner**
463 **E, Ghany M, and Bonner RF.** Laser capture microdissection of single cells from
464 complex tissues. *Biotechniques* 26: 328-335, 1999.
- 465 22. **Taguchi M, and Otsuki M.** Co-localization of nestin and PDX-1 in small
466 evaginations of the main pancreatic duct in adult rats. *J Mol Histol* 35: 785-789,
467 2004.
- 468 23. **Taguchi M, Yamaguchi T, and Otsuki M.** Induction of PDX-1-positive cells in
469 the main duct during regeneration after acute necrotizing pancreatitis in rats. *J*
470 *Pathol* 197: 638-646, 2002.
- 471 24. **Yamaguchi J, Liss AS, Sontheimer A, Mino-Kenudson M, Castillo CF,**
472 **Warshaw AL, and Thayer SP.** Pancreatic duct glands (PDGs) are a progenitor
473 compartment responsible for pancreatic ductal epithelial repair. *Stem cell*
474 *research* 15: 190-202, 2015.
- 475

476 **SUPPLEMENTAL DATA**

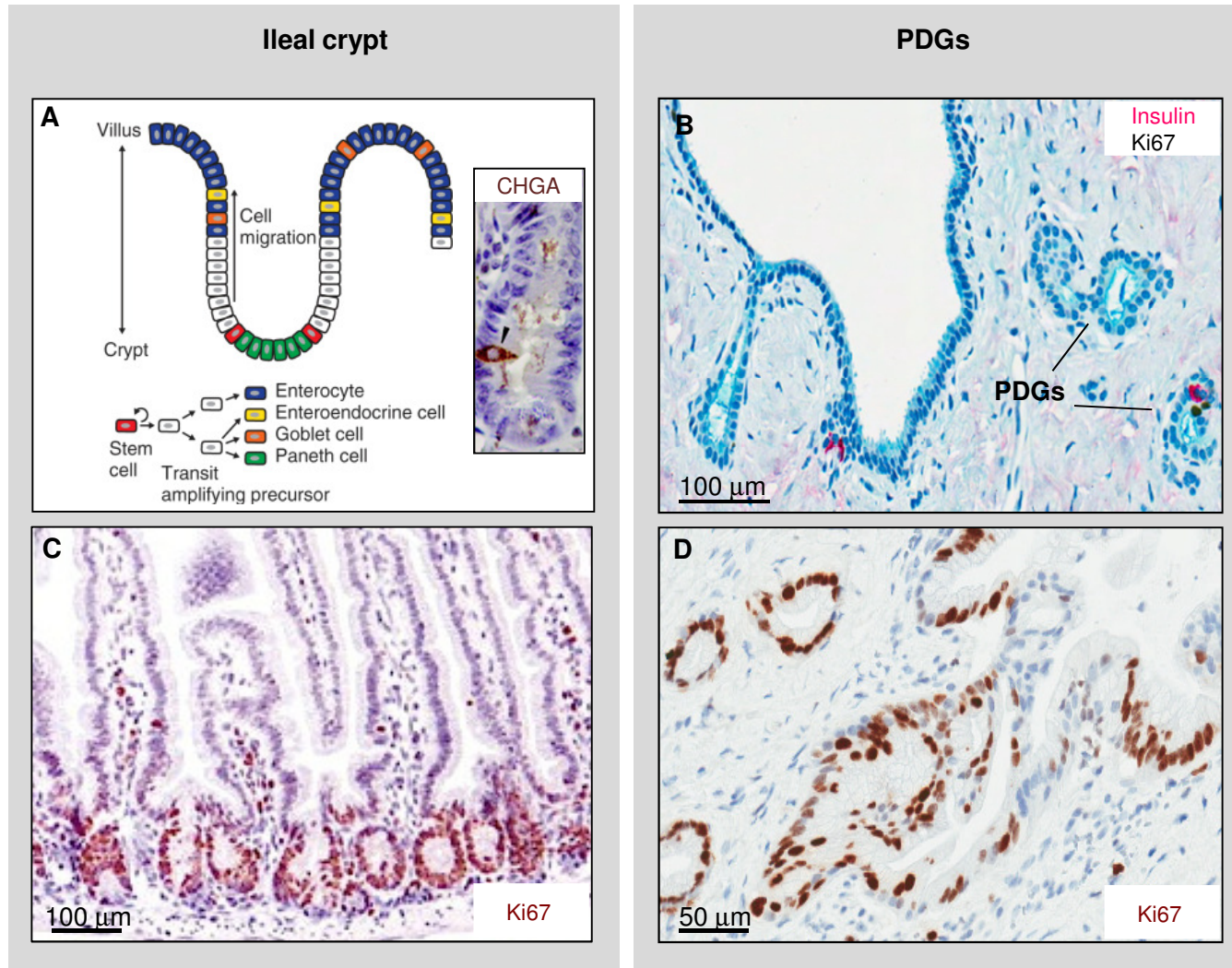
477 **Table 1:** List of 22 differentially expressed genes when comparing the 6 PDG samples
478 vs. the average expression levels across 84 human samples in the Human GNF
479 database. Fold changes are expressed after log2 transformation.

480

481 **Table 2:** List of 245 differentially expressed genes when comparing the PDG samples
482 from the HIP rat model of type 2 diabetes vs. WT animals. Fold changes are expressed
483 after log2 transformation.

484

Figure 1



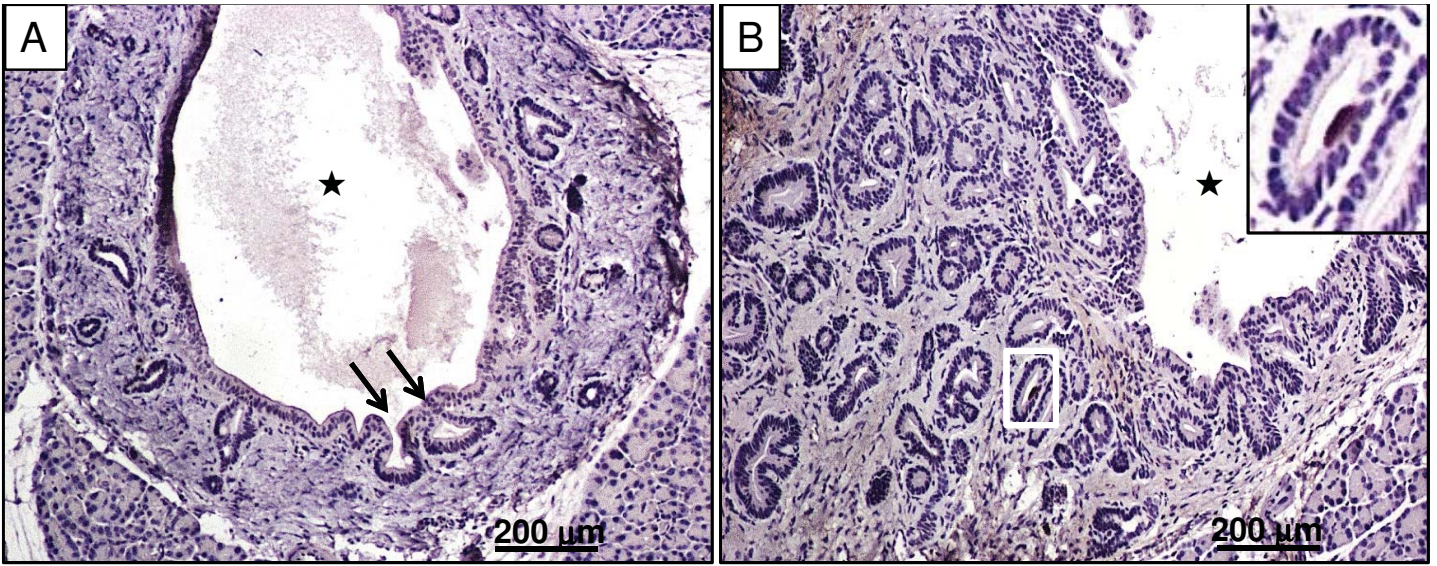


Figure 2

